A coral-based reconstruction of sea surface salinity at Sabine Bank, Vanuatu from 1842 to 2007 CE

Meaghan K. Gorman,[1,2] Terrence M. Quinn,[1,2] Frederick W. Taylor,[1] Judson W. Partin,[1] Guy Cabioch,[3,4] James A. Austin Jr.,[1] Bernard Pelletier,[5] Valérie Ballu,[6] Christophe Maes,[7] and Steffen Saustrup[1]

[1]   Climate variability associated with the El Niño Southern Oscillation (ENSO) results in large sea-surface temperature (SST) and sea-surface salinity (SSS) anomalies in many regions of the tropical Pacific Ocean. We investigate interannual changes in SSS driven by ENSO in the southwestern Pacific at Sabine Bank, Vanuatu (SBV, 166.04°E, 15.94°S) using monthly variations in coral $\delta^{18}O$ from 1842 to 2007 CE. We develop and apply a coral $\delta^{18}O$-SSS transfer function, which is assessed using a calibration-verification exercise (1970–2007 CE). The 165-year reconstructed SSS record contains a prominent trend toward freshening from 1842 to 2007 CE; mean SSS for 1842–1872 CE is 35.46 ± 0.28 psu, which contrasts with a mean value of 34.85 ± 0.31 psu for 1977–2007 CE, with a freshening trend during the latter part of the 20th century that is not unprecedented with respect to the overall record. Variance in the record is concentrated in the interannual (42%) and interdecadal (29%) bands. The SBV-SSS record matches well with a similarly reconstructed SSS time series at Malo Channel, Vanuatu, which is located ∼120 km to the east of SBV. This regional signal is likely driven by ENSO-related changes in the SPCZ and interdecadal changes in surface water advection. The pattern of interdecadal variability at SBV agrees reasonably well with coral records of interdecadal variability from Fiji and Tonga, especially in the pre-1940 portions of the records, further evidence for the regional extent of the salinity signal at Sabine Bank, Vanuatu.

1.   Introduction

[2]   The El Niño Southern Oscillation (ENSO) is a coupled ocean-atmosphere phenomenon that results in sea surface temperature (SST) and salinity (SSS) anomalies throughout the tropical Pacific Ocean, changes in atmospheric circulation, and many additional teleconnections worldwide on interannual timescales [*Bjerknes* 1969; *Rasmusson and Carpenter*, 1982; *Ropelewski and Halpert*, 1987]. A better understanding of the future behavior of the ENSO system requires an improved understanding of its natural variability in the past. ENSO can be recognized in records of SST and SSS anomalies (SSTA and SSSA, respectively, e.g., 1997–98, 1982–83, 1972–73), but instrumental records of SST and SSS are often insufficient in spatial and temporal coverage to address issues related to long-term variability. Gridded SST products extend back into the nineteenth century, but are more reliable in the latter half of the twentieth century, in part due to better temporal and spatial coverage [*Rayner et al.*, 2006]. Tropical SSS records remain rare; those that exist extend back only to 1950, and the interval from 1970 to present is characterized by the most robust measurements due to increased number of observations [*Delcroix et al.*, 2011]. SSS information is also available from data assimilation products [e.g., *Carton and Giese*, 2008].

[3]   ENSO variability also results in changes in the location of the South Pacific Convergence Zone (SPCZ), a region of heavy precipitation extending southeast from

---

[1]Institute for Geophysics, Jackson School of Geosciences, University of Texas at Austin, Austin, Texas, USA.
[2]Department of Geological Sciences, Jackson School of Geosciences, University of Texas at Austin, Austin, Texas, USA.
[3]UMR LOCEAN, Institut de Recherche pour le Développement, Bondy, France.
[4]Deceased 28 October 2011.
[5]UMR GEOAZUR, Institut de Recherche pour le Développement, Nouméa, New Caledonia.
[6]Université Paris Diderot, PRES Sorbonne Paris Cité, IPGP/UMR CNRS 7154, Paris, France.
[7]UMR LEGOS, Institut de Recherche pour le Développement, Nouméa, New Caledonia.

Corresponding author: M. K. Gorman, Department of Geological Sciences, Jackson School of Geosciences, University of Texas at Austin, 1 University Dr., C1100, Austin, TX 78712, USA. (mkgorm@utexas.edu)

Central Pacific El Niño
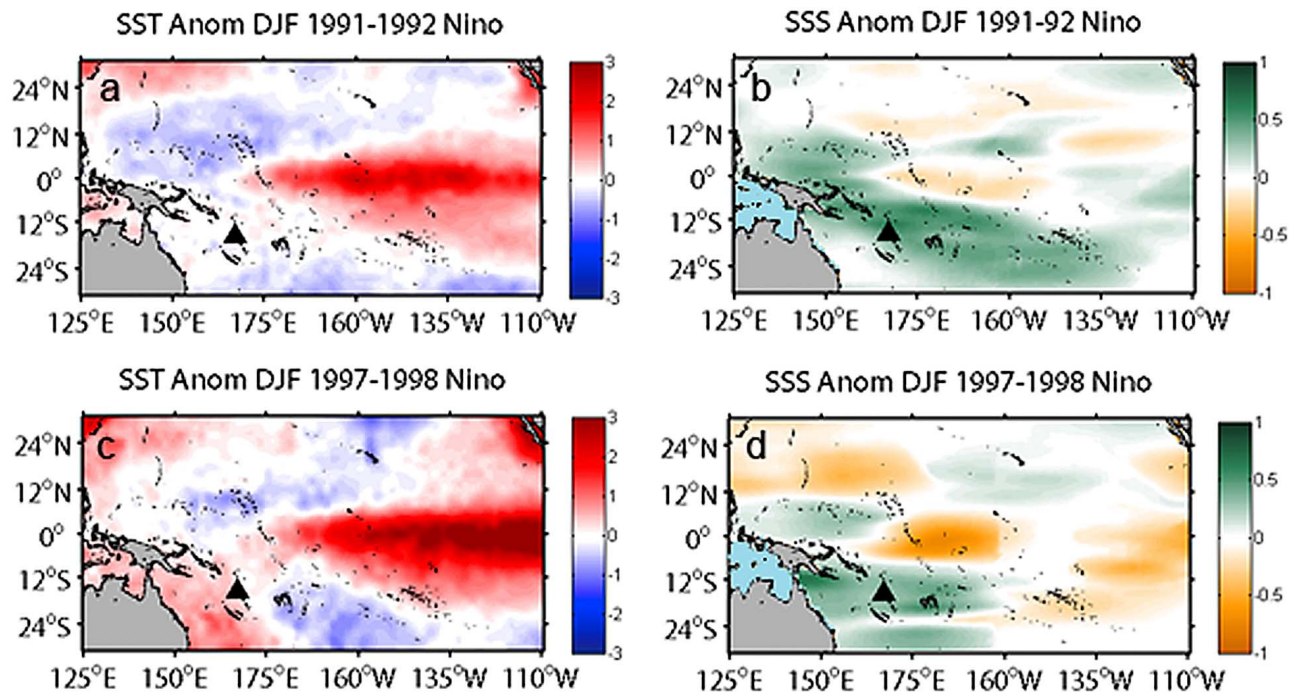

Eastern Pacific El Niño

Figure 1. (left) SSTA and (right) SSSA in the tropical Pacific during the (a, b) 1991–1992 and (c, d) 1997–1998 ENSO warm-phase events, during the months December, January, and February (DJF), when the amplitude of an ENSO event is at its peak. Both events appear as a strong SSSA in the instrumental record, as well as in our reconstructed SSS record at Vanuatu (black triangle). The 1991–1992 event is identified as a central Pacific warm-phase event, and the 1997–1998 is identified as an eastern Pacific warm-phase event, both of which manifest in SSTA and SSSA in similar ways at Vanuatu. Given these plots, the SSSA response to ENSO at Vanuatu exceeds the SSTA response, a relationship that should also be manifest in the coral $\delta^{18}O$ record.

Papua New Guinea in the southwest Pacific which is crucial to summertime circulation in the Southern Hemisphere [*Kiladis et al.*, 1989]. ENSO-influenced movement of the SPCZ causes interannual variability in the hydrologic balance of this region (precipitation-evaporation (P-E) balance), affecting salinity in surface ocean waters. The SPCZ shifts to the northeast (southwest) during an ENSO warm (cool) phase event, which results in less (more) rainfall at Vanuatu, and therefore increased (decreased) salinity [*Folland et al.*, 2002; *Juillet-Leclerc et al.*, 2006]. The movement of the SPCZ also results in oceanographic changes in the southwest Pacific. A salinity front, which has a mean position of ∼175°W, 15°–20°S and separates higher salinity waters to the east from lower salinity waters (under SPCZ) to the west, migrates east-west during ENSO events. This movement is partly due to a change in the P-E balance, and partly due to zonal advection [*Gouriou and Delcroix*, 2002]. During a warm (cool)-phase event, the salinity front shifts to the southeast (northwest), moving farther away from (closer to) Vanuatu, tracking the movement of the SPCZ during these events.

[4] Decadal-scale variability has also been observed in the tropical Pacific [*Evans et al.*, 2001; *Linsley et al.*, 2000, 2006, 2008; *Mantua et al.*, 1997; *Power et al.*, 1999]. One

mechanism proposed to be responsible for such variability is changes in subtropical cells (STC) [*McCreary and Lu*, 1994]. These STCs establish a link between the tropical and subtropical oceans, in which water with an anomalous SST signature subducts in the subtropics, travels along the pycnocline toward the equator and upwells in the tropics, affecting the SSTs and overlying atmospheric circulation [*Gu and Philander*, 1997; *McPhaden and Zhang*, 2002; *Zhang and McPhaden*, 2006]. Alternatively, it has been suggested that ENSO variability and atmospheric noise may sum to produce the observed Pacific decadal variability [*Newman et al.*, 2003]. More long proxy records of decadal-scale variability in the tropics, such as the one presented here, are needed to further investigate this mode of variability.

[5] Sabine Bank (SBV) is located in the Republic of Vanuatu, an island chain located in the southwest Pacific at the southern edge of the Western Pacific Warm Pool (WPWP) and under the SPCZ. The bank sits ∼78 km offshore from and to the west of the nearest island of Espiritu Santo, making it a truly 'open ocean' site. During ENSO warm-phase events, SSTA at Vanuatu are modest relative to many other regions of the tropical Pacific (Figures 1a and 1c). In contrast, SSSA during ENSO warm-phase events are
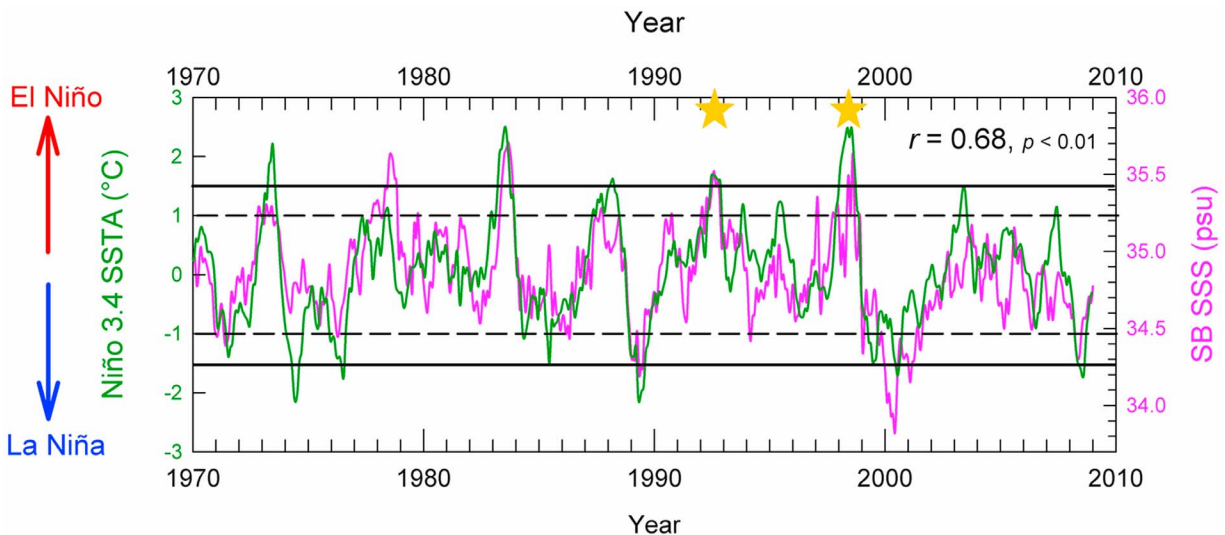
Figure 2. Niño 3.4 SSTA (green) compared to SSS (pink) extracted from the grid box containing Sabine Bank, Vanuatu (SBV), over the period 1970–2007 CE. A maximum correlation ($r = 0.67$; $p < 0.01$) between the time series is reached when Vanuatu SSS lags Niño 3.4 SSTA by 6 months, but the correlations are strong (>0.60) for lags of 4 to 8 months. The lagged response of SSS in the western Pacific region relative to changes in SSTA in the Niño 3.4 region is also noted in models and observations [*Delcroix et al.*, 2011]. The strong correlation between these records reflects a dynamical link between SSS at SBV and ENSO, demonstrating that ENSO variability drives SSS variations at SBV. ENSO warm (cold)-phase events manifest as warm (cold) anomalies in the Niño 3.4 region, and as positive (negative) salinity anomalies at Vanuatu. We expect that ENSO events will manifest as similar SSS excursions in the proxy-based SSS reconstruction. Horizontal dashed lines indicate a threshold for which moderate events are defined and the horizontal solid lines indicate a threshold for which strong events are defined in the Niño 3.4 region. ENSO events discussed in Figure 1 are represented here by gold stars.

enhanced toward positive values in the southwest Pacific compared to many other locations throughout the tropical Pacific (Figures 1b and 1d). A comparison of Niño 3.4 SSTA (canonical ENSO signal) with SBV SSS demonstrates a dynamical link between ENSO and the SSS signal at SBV (Figure 2); a maximum correlation (0.67; $p < 0.01$) between the time series is reached when SBV SSS lags Niño 3.4 SSTA by 6 months. *Delcroix et al.* [2011] have noted that a similar lag relationship is observed in models and observations. This suggests that SSS variability is driven by ENSO changes on interannual time scales. The central tropical Pacific is recognized as a 'center of action' in terms of the SST response to ENSO forcing; however, the southwest tropical Pacific is marked by its strong SSS response to ENSO forcing.

[6] SST and SSS variability associated with ENSO and SPCZ variability are recorded as changes in coral δ^{18}O, as these values reflect the combined influence of ambient variations in SST and seawater δ^{18}O values ($\delta^{18}O_{SW}$) [e.g., *Cole and Fairbanks*, 1990; *McConnaughey*, 1989; *Weber and Woodhead*, 1972]. Coral δ^{18}O has long been recognized as a proxy for SST [*Fairbanks and Matthews*, 1978; *Dunbar and Wellington*, 1981; *Quinn et al.*, 1998], but deconvolving the $\delta^{18}O_{sw}$-SSS signal has been a difficult task, due to the paucity of instrumental SSS records for comparison. This challenge has severely limited the attempts at using δ^{18}O to reconstruct SSS. Some studies have demonstrated a strong δ^{18}O–SSS correlation [e.g., *Cole and Fairbanks*, 1990; *Le Bec et al.*, 2000], but actual SSS reconstructions are limited

[*Juillet-Leclerc et al.*, 2006; *Delcroix et al.*, 2011]. The SBV salinity reconstruction presented here is greatly facilitated by the recent development of a $1° \times 1°$ gridded SSS data set [*Delcroix et al.*, 2011], which permits the establishment of a direct link between SSS variations and coral δ^{18}O variations at SBV. We compared the *Delcroix et al.* [2011] data set to the Simple Ocean Data Assimilation (SODA) reanalysis data set [*Carton and Giese*, 2008] and found a modest correlation of 0.39, $p < 0.05$, indicating a shared variance between the two data sets of only 15%. The SSS data set of *Delcroix et al.* [2011] is ideal for our location, because the ship of opportunity track (New Caledonia-Japan route) passes very near Sabine Bank, resulting in more accurate SSS measurements than for locations farther from such ship tracks. In this paper, we also demonstrate that the δ^{18}O-salinity relationship at SBV is regional in extent.

2. Methods

[7] A 2-m long core (06SB-A1) was extracted from a *Porites lutea* coral head in 8 m of water at Sabine Bank, Vanuatu (166.07°E, 15.94°S), in December 2006. A 2.9-m long core (07SB-A2) was extracted from the same coral head in October 2007, reaching the base of the coral. We prepared the 8-cm diameter cores by cutting them into 6-mm thick slabs; X-radiographs of these slabs helped to determine the maximum growth axis of the coral, which guided the selection of the most appropriate sampling paths for micromilling powders. Using a computer assisted micromill drilling system, we collected coral sample powders at 1 mm intervals,

which equates to approximate monthly sampling, given an estimate of an annual extension rate of 1.2 cm/yr. Core 06SB-A1 was sampled in its entirety and 07SB-A2 was sampled from 0 to 40 cm (to confirm overlap of the two cores and to gain an extra year in the time series) and from 143 to 290 cm, which overlaps with the lower end of 06SB-A1 and extends the time series back to 1842 CE. Results are only reported to a depth of 200 cm as a result of diagenetic alteration at the bottom of the core, which is visible as dark patches in the X-radiographs and large excursions, as well as the lack of an annual cycle in the geochemical time series.

[8] Stable isotope determinations were made on aliquots of sample powder using a Thermo-Finnigan MAT253 Isotope Ratio Mass Spectrometer (IRMS), with a Kiel IV Carbonate Device, and on a Thermo-Finnigan Delta V Plus IRMS with Gasbench II (GB II) connected to a Conflo IV, both at the Analytical Laboratory for Paleoclimate Studies (ALPS) at the Jackson School of Geosciences, University of Texas at Austin. The precision of the Kiel IV/MAT253 IRMS for samples in this study is 0.05‰ for $\delta^{18}O$ and 0.03‰ for $\delta^{13}C$ (1σ), as estimated via multiple analyses of a carbonate standard (n = 224), which is consistent with long-term precision for this instrument of 0.06‰ for $\delta^{18}O$ and 0.03‰ for $\delta^{13}C$. The precision of the GB II/Delta V Plus IRMS is 0.07‰ for $\delta^{18}O$ and 0.03‰ for $\delta^{13}C$ (1σ), as estimated via multiple analyses of the same carbonate standard (n = 25), which is consistent with long-term precision for this instrument of 0.07‰ for $\delta^{18}O$ and 0.03‰ for $\delta^{13}C$. Replicate coral samples analyzed on both mass spectrometers yield similar results (mean difference = 0.03‰ for $\delta^{18}O$ and 0.12‰ for $\delta^{13}C$; n = 35). All stable isotope values are reported relative to Vienna Pee Dee Belemnite (VPDB), in standard delta notation.

[9] Geochemical variations versus depth were converted to variations versus time using AnalySeries software [Paillard et al., 1996]. Geochemical variations in $\delta^{18}O$ were used to determine a first-order age model, with the maximum intra-annual peaks in $\delta^{18}O$ being assigned as the coldest month of the year (August), beginning with the year 2007, when the living coral was cored. This first-order age model places $\delta^{18}O$ variations in the time domain, with uneven time increments (Δt). A second-order age model, with a monthly Δt, was created using the AnalySeries software program, which was verified by comparing years with anomalous $\delta^{18}O$ values to known ENSO events where possible. This second-order age model is the final age model used in all plots and data analysis.

[10] Statistical comparisons between coral proxy variations and instrumental variations were performed in anomaly space to avoid the problem of serial autocorrelation in time series with such strong annual cyclicity ($\gamma = 0.96$). Anomalies are calculated as deviations from the monthly climatology of each variable between 1961 and 1990 CE, a time interval selected in order to compare all data sets (including the comparison site, Malo Chanel, which only extends to 1991 CE) using the same base period. Despite the smaller number of observations in SSS data prior to 1970 CE, comparison of the SSS base period from 1961 to 1990 CE to the period 1971–2000 CE showed no significant difference, hence 1961–1990 was chosen to accommodate all records. A 6-month lag in Vanuatu SSS was used in the

comparison between SSS and Niño 3.4 SSTs [Kilbourne et al., 2004].

[11] Thermistor logger data were collected at SBV from 2000 to 2006 CE, allowing a direct comparison of 6 years of daily in situ data with gridded products and coral geochemistry (Figure 3). The amplitude of the annual cycle in the in situ SST time series is slightly larger ($\sim 0.5^\circ C$) relative to the SST time series extracted from the gridded SST product, but otherwise the two records are similar. SSS has a weaker annual cycle at SBV relative to SST. We note overall good agreement between in situ SSS and gridded SSS time series as well ($r = 0.69$, $p < 0.01$). The good agreement between in situ data and data extracted from gridded products provides additional confidence in relationships derived between proxy and environmental data outside of the 2000–2006 CE period of overlap in the records.

[12] We determined the error associated with the long-term trends in $\delta^{18}O$, $\delta^{13}C$, and SSS by fitting a trend through the data and using errors in the X and Y variables to determine an equation with error in the slope and intercept. Combining these two errors resulted in the errors on all of the trends discussed. This takes into account analytical error and error associated with age modeling.

3. Results and Discussion

[13] The monthly resolved SBV coral $\delta^{13}C$ and $\delta^{18}O$ time series show strong annual cyclicity, as well as a long-term trend toward more negative values from 1842 to 2007 CE (Figure 4). Over the length of the record, mean coral $\delta^{18}O$ values decrease by 0.41 ± 0.16 ‰, whereas mean coral $\delta^{13}C$ values decrease by 0.74 ± 0.41‰. Major ENSO events identified in the instrumental and historical records (e.g., 1997–98, 1972–73, 1941–42, 1887–88) are recorded in the SBV coral record as large $\delta^{18}O$ excursions, which are especially prominent (>0.2 ‰) in the $\delta^{18}O_{anomaly}$ time series, where the annual cycle has been removed to more clearly highlight lower frequency variability. The cause of coral $\delta^{13}C$ variations remains poorly understood, but many factors have been suggested, including the $\delta^{13}C$ signature of the DIC in ocean water, which is related to reef productivity, coral geometry and extension rate, and rates of photosynthesis and respiration [e.g., Weber and Woodhead, 1971; Land et al., 1975; McConnaughey, 1989; Bacastow et al., 1996; Swart et al., 2005]. We choose not to interpret the coral $\delta^{13}C$ signal in this study, because it does not unambiguously address our objectives.

[14] We performed singular spectrum analysis (SSA) on the $\delta^{18}O_{anomaly}$ time series (Figure 5a) to investigate variability in the record, as a function of frequency. Results of the analysis indicate that 42% of the variance in the $\delta^{18}O_{anomaly}$ time series is concentrated in the interannual (2–6 years) frequency band (Figure 5b), which is consistent with ENSO forcing of the coral $\delta^{18}O$ record. There is also a large concentration of variance in the $\delta^{18}O_{anomaly}$ time series (29%) in the interdecadal (14 years) band (Figure 5d), which matches well with the mean state, or the average $\delta^{18}O$ values calculated for 6 year bins (Figure 5c). Singular Spectrum Analysis (SSA) indicates that there are periods of high interannual variability at the same time as quiescence in the interdecadal band (i.e., 1960–2000 CE), suggesting a decoupling of the mechanisms behind these two periods of variability. The
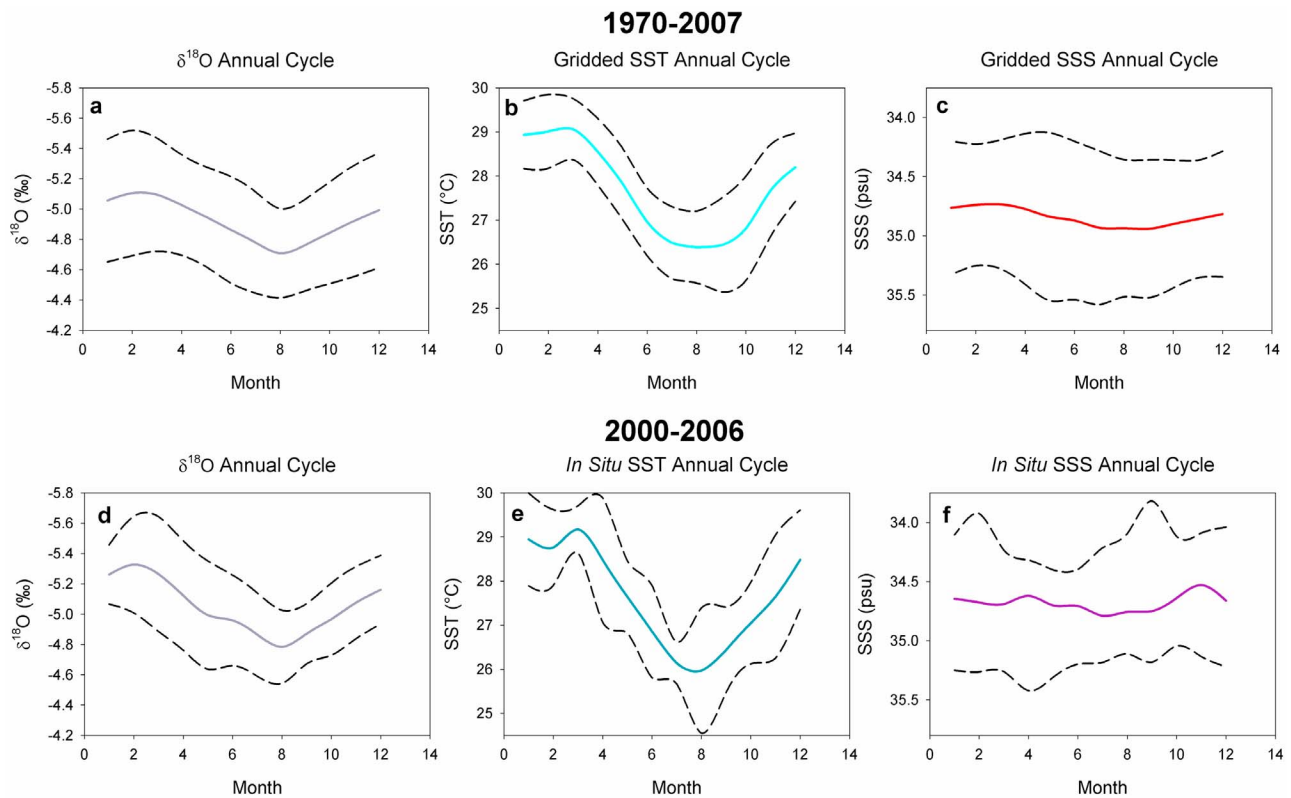
1970-2007

2000-2006

Figure 3. The average annual cycle at SBV in (a, d) coral $\delta^{18}O$ (gray); (b) gridded SST (light blue); (c) gridded SSS (red); (e) in situ SST (teal); and (f) in situ SSS (purple; 2000–2006 CE). Figures 3a–3c are calculated over the period 1970–2007 CE (length of gridded SSS data), and Figures 3d–3f are calculated over the period 2000–2006 CE (length of in situ data). Dashed lines represent the 2σ standard deviation on the respective annual cycles. Gridded products and in situ data are the same within error. The $\delta^{18}O$ and SST variations both show pronounced annual seasonality, whereas SSS variations do not. The relatively small standard deviation in SST contrasts with the larger standard deviation in SSS, suggesting the presence of a pronounced super-annual signal in SSS. The coral $\delta^{18}O$ signal records both SST and SSS changes; hence, the expectation of a strong SST component in the sub-annual band, with a strong SSS component in the super-annual band. Furthermore, a coral $\delta^{18}O$ anomaly record, which removes the influence of the annual cycle, should act to isolate the super-annual signal in SSS.

large concentration of variance in the interdecadal band leads us to investigate the possible mechanisms behind this period of variability, which is currently not well understood in the tropical Pacific.

3.1. Assessing the Influence of Temperature and Salinity on the Coral $\delta^{18}O_{anomaly}$ Record

[15] We used gridded SST and SSS products to develop a pseudocoral, or modeled coral $\delta^{18}O$ [*Brown et al.*, 2008; *Thompson et al.*, 2011], that represents the expected $\delta^{18}O_{anomaly}$ record given the instrumental SSTA and SSSA in the region (Figure S1 in the auxiliary material), in order to investigate the contributions of temperature and salinity to the coral $\delta^{18}O_{anomaly}$ signal.[1] The pseudocoral was calculated by converting instrumental SST and SSS for Sabine Bank [*Rayner et al.*, 2003; *Delcroix et al.*, 2011], using a

standard $\delta^{18}O$-SST calibration of $-0.21‰/°C$ [*DeLong et al.*, 2010] and a $\delta^{18}O$-SSS calibration of 0.38 ‰/psu (determined relationship for this record using the in situ and $\delta^{18}O$ data, falls between the observed 0.27 to 0.42 ‰/psu range for the tropical Pacific [*Fairbanks et al.*, 1997; *Morimoto et al.*, 2002]). We compared our observed $\delta^{18}O$ anomaly record with three versions of the pseudocoral: the combined influence of SST and SSS (total pseudocoral), SST alone, and SSS alone to examine the contribution of each to the coral $\delta^{18}O_{anomaly}$ record. We found that the correlations with $\delta^{18}O$ are 0.72 (with total pseudocoral), 0.47 (with SST component), and 0.68 (with SSS component), $p < 0.01$ for all three (Figure S1), indicating that SSS changes represent a larger fraction of the variance in the coral $\delta^{18}O_{anomaly}$ signal than SST changes, as expected from the larger magnitude of interannual SSS variations at this site. Testing several different percent contributions of SSS and SST to create the pseudocoral, we determined that a combination of 35% SST and 65% SSS results in the closest representation to the
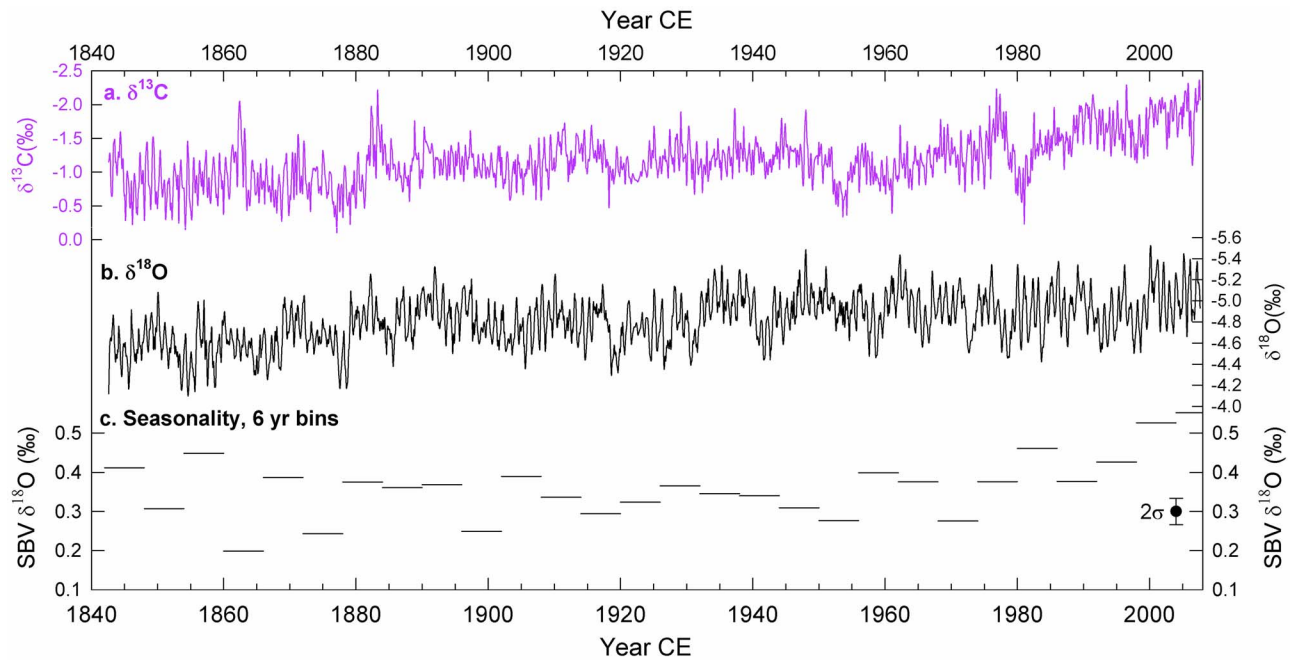
Figure 4. Stable isotopic time series from SBV coral from 1842 to 2007 CE (a) δ^{13}C (purple), (b) δ^{18}O (black). There is a strong annual cycle in both time series, as well as a trend of -0.41 ± 0.16 ‰ for coral δ^{18}O and -0.74 ± 0.41‰ for δ^{13}C toward depletion in the raw time series. (c) The annual cycles (calculated as the range of each 6-year bin) shows periods of high variability ($\sim$1840–1910, 1960–2007 CE) and periods of low variability ($\sim$1910–1960). The average annual cycles for each 6-year bin can be seen in Figure S4.

observed coral δ^{18}O$_{anomaly}$ values. This was calculated by creating a pseudocoral that consisted of percent SST/SSS contributions that ranged from 100/0% to 0/100%, in increments of 5% (i.e., 100/0, 95/5, 90/10… 5/95, 0/100). The pseudocoral consisting of 35/65% gave the highest correlation with the measured δ^{18}O time series, which provides the percent contributions of SST and SSS to the time series. This relationship was determined over the period 1970–2007, and is limited by the length of the instrumental SSS data set. We assume stationarity in the proportional contributions of SST and SSS to the coral δ^{18}O signal because SSS data needed to evaluate this assumption are lacking in the pre-1970 period. However, the assumption of stationarity of a proxy-instrumental relationship developed over the instrumental time period affects all proxy-based climate reconstructions that extend beyond the instrumental period. Thus, lacking additional instrument data and/or another independent SST- or SSS-only proxy there is no easy way to reduce the uncertainty of the empirically derived proxy relationship over the calibration-verification interval.

[16] The long-term depletion in the coral δ^{18}O$_{anomaly}$ record is -0.41 ± 0.16 ‰. Given our calculated percent contributions, the resultant SST trend is a warming of $0.68 \pm 0.76°$C, which is statistically the same as the gridded SST record from this region, which suggests a $\sim$0.45 $\pm$ 0.45°C warming since 1870 CE. We attribute the remainder of the trend to an SSS freshening, which equates to $\sim$0.70 $\pm$ 0.42 psu freshening since 1842 CE. We note that salinity is reported in regular intervals with a resolution of 0.01 pss-78, according to the 1978 practical salinity scale.

We use the simplified 'psu' for practical salinity units [*Reverdin et al.*, 2012].

3.2. Development and Testing of the Coral δ^{18}O$_{anomaly}$-SSS Transfer Function at SBV

[17] We develop and test a transfer function constructed using linear regression analysis of SBV coral δ^{18}O$_{anomaly}$ variations and instrumental SSS over the period 1970–2007 CE [*Thirumalai et al.*, 2011]. The equation of that function is

$$SSS = (34.861 \pm .007) + (1.772 \pm .048) * \delta^{18}O_{anomaly};$$
$$r = 0.66; p < 0.01 \tag{1}$$

We performed a calibration-verification exercise (Figure 6) between δ^{18}O$_{anomaly}$ and SSS at SBV to assess the robustness of the transfer function [*Quinn and Sampson*, 2002]. The relationship between coral δ^{18}O$_{anomaly}$ and salinity in the calibration interval (1988–2007 CE) is

$$SSS = (34.880 \pm 0.011) + (1.973 \pm 0.076) * \delta^{18}O_{anomaly};$$
$$r = 0.65; p < 0.01 \tag{2}$$

whereas this relationship in the verification interval (1970–1987 CE) is

$$SSS = (34.855 \pm .010) + (1.616 \pm .065) * \delta^{18}O_{anomaly};$$
$$r = 0.65; p < 0.01 \tag{3}$$
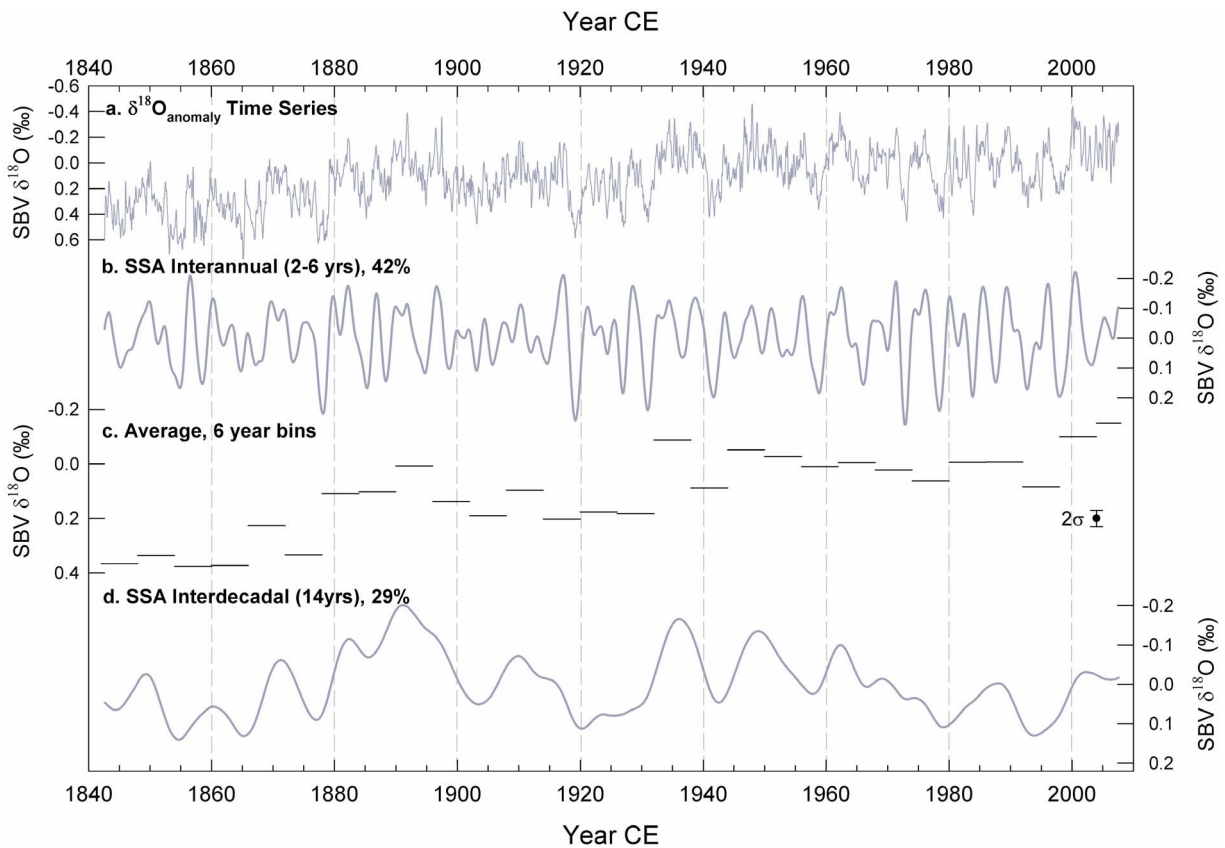
Figure 5. (a) SBV coral $\delta^{18}O_{anomaly}$ time series; (b) Singular Spectrum Analysis (SSA) reconstruction of interannual variability, which accounts for 42% of the variance in the coral $\delta^{18}O_{anomaly}$ record; (c) average value of the 6 year bins presented in Figure 4;, and (d) SSA reconstruction of interdecadal variability, which accounts for 29% of the variance in the record. Periods of enhanced interannual variability (Figure 5b) appear to coincide with periods of somewhat quiescent interdecadal variability (Figure 5d), i.e., 1960–2000 CE, indicating a decoupling of processes controlling the variability on these two time scales. Interdecadal variability coincides well with the changes in 6 year binned averages, or the mean state, except for the latter part of the record, ~1980–2007 CE.

The slopes in equations (1)–(3) are within error of each other; however, the intercepts are slightly different. Despite this small difference, the similarity of the lines (Figure S2) provides confidence that the transfer function developed in this study can be used to reconstruct past changes in salinity at this locality based on coral $\delta^{18}O$ variations. We also note that there is a signal in the residuals, which likely reflects a small temperature component in the coral $\delta^{18}O$ anomaly signal (Figure 6, bottom), most likely due to the small changes in seasonality over this time period (Figure 4c).

[18] We applied the calibration interval equation (2) and the verification interval equation (3) to the same $\delta^{18}O_{anomaly}$ values from SBV over the period 1970–2007 CE, resulting in an average misfit between the two data sets of 0.08 ± 0.06 (1σ) psu. We also calculated the average of the absolute value of the misfit between the reconstructed and instrumental SSS and found it to be 0.20 ± 0.15 (1σ) psu. These two error estimates provide a means to estimate error in paleo-salinity reconstructions, the latter of which is used for a conservative error estimate on the SSS reconstruction presented here.

3.2.1. Reconstructed SSS Variations at SBV From 1842 to 2007 CE: Long-Term Trend

[19] The reconstructed SSS time series at SBV (Figure 7) has a prominent trend (0.70 ± 0.42 over the length of the record) toward freshening from 1842 to 2007 CE when the 65% SSS contribution is taken into account. When the trend in the reconstructed SSS time series is corrected to 0.70 ± 0.42 psu, it is within error of the original time series (gray 1σ error cloud, Figure 7, trend of 1.08 ± 0.42 psu); therefore, the trend information in the initial time series resulting from the $\delta^{18}O$-SSS transfer function is preserved. The trend over the period 1970–2007 is observed to be -0.19 psu in the gridded data set, while the reconstructed SSS trend over this period is -0.31 ± 0.05 psu, which is different than observed, likely due to the averaging of the instrumental SSS record over a $1° \times 1°$ grid square. This value for the period 1970–2007 has been converted to the rate of freshening per decade to compare with other records, resulting in a calculation of 0.08 ± 0.05 psu/decade freshening. The freshening recorded in the SBV coral agrees with the 0.07 psu/decade observed in this region of the WPWP
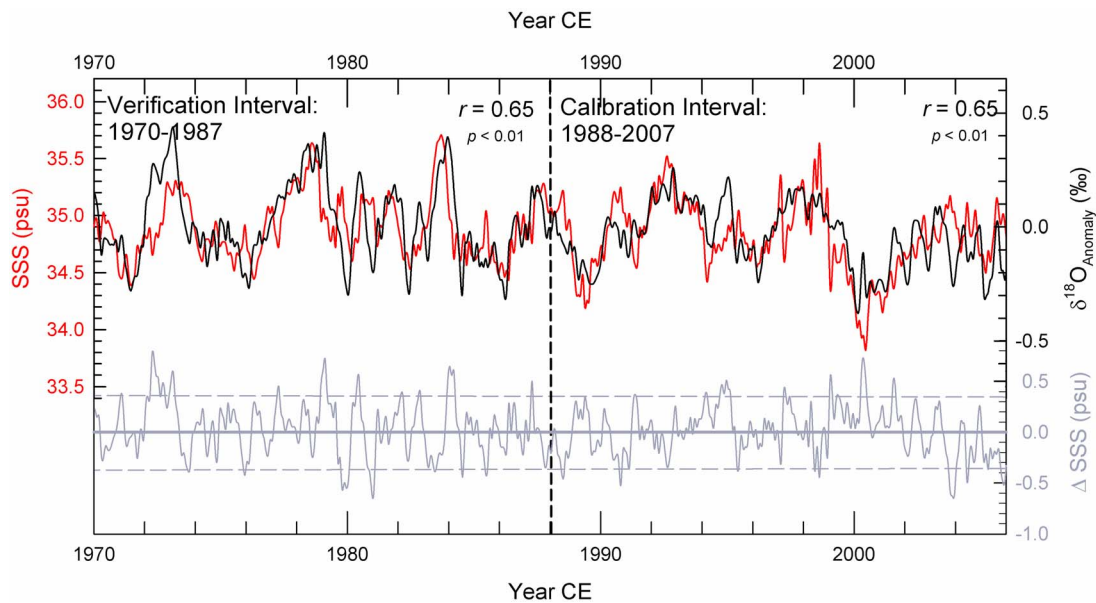
Figure 6. (top) A calibration-verification exercise was used to assess the relationship between variations in coral $\delta^{18}O_{anomaly}$ (black line) and SSS (red line) at Vanuatu. A linear transfer function between coral $\delta^{18}O$ and SSS was developed over the calibration period (1988–2007) and applied to the verification period (1970–1987); a transfer function developed for the verification period was applied to the calibration period. We compared both to the instrumental SSS record (red) and the same correlation ($r = 0.65$, $p < 0.01$) was observed over both time intervals, indicating that the $\delta^{18}O$-SSS relationship is stationary over this period. (bottom) The difference between the instrumental and reconstructed SSS, with dashed horizontal lines indicating the 1σ error associated with the salinity reconstruction (±0.35 psu).

[*Cravatte et al.*, 2009], and the freshening of 0.04 to 0.10 psu/decade observed throughout the western tropical Pacific [*Delcroix et al.* 2007]. This observed freshening may be explained by a shift in the P-E balance of the region, predicted as increased evaporation, increased moisture in the atmosphere, and increased precipitation in convective regions due to a warming climate [*Held and Soden*, 2006; *Vecchi et al.*, 2006]. The migration of the salinity front associated with the SPCZ to the south and east [*Cravatte et al.*, 2009] may also be a factor contributing to the observed freshening. *Singh and Delcroix* [2011] have examined whether freshening in the western tropical Pacific may be due to an increase in ENSO events or climate change, and have determined that the driver of freshening is climate change, as described above, providing additional confidence in our proposed freshening mechanism.

3.2.2. Reconstructed SSS Variations at SBV From 1842 to 2007 CE: ENSO

[20] We further explore the response of SSS variations at SBV to ENSO forcing documented in the instrumental record (Figure 2) by evaluating the skill of the coral salinity proxy at SBV with known ENSO events, identified in the instrumental SST record in the Niño 3.4 region, back to 1870 CE. We use an algorithm developed by *Hereid et al.* [2010], which calculates an ENSO event threshold definition, to perform this assessment. The threshold is selected where the proxy maximizes accuracy, while minimizing errors (falsely identified events plus missed events). A threshold of ±0.06‰ has been determined from the ENSO-filtered $\delta^{18}O$ time series from SBV. We consider it acceptable to use this small value as a threshold, because it is an

order of magnitude larger than the value that the analytical error takes on once the time series is filtered, which is determined by a Monte Carlo analysis of 1,000 filtered records of the original time series with varying amounts of analytical error. The percentage of known events that are correctly identified provides a measure of coral proxy skill. The SBV coral proxy correctly identifies 63% of El Niño events and 59% of La Niña events over the instrumental record. While not perfect, this skill level provides a means by which to assess the ENSO occurrences in the pre-instrumental period.

[21] The SBV monthly resolved, proxy-based SSS reconstruction (Figure 7) captures the salinity response to the major ENSO warm phase events recognized in instrumental records (El Niño, e.g., 1997–98, 1972–73, 1941–42), and several negative salinity excursions associated with ENSO cool-phase events (La Niña, e.g., 1998–2001, 1973–76). The 1972–73 ENSO warm-phase event is captured in the coral $\delta^{18}O_{anomaly}$ record as a strong SSS anomaly – stronger in fact than that observed in the instrumental SSS record. This interval of the instrumental SSS record is marked by fewer observations, and hence it is possible that the magnitude of the SSS event is underestimated in the instrumental SSS record. Perhaps more importantly, the SBV coral proxy SSS record captures the major ENSO warm phase events of 1877–78, 1918–19, and 1941–42, which are also observed as anomalous in the instrumental SST record, but that occur prior to the beginning of the instrumental SSS record. The SSS reconstruction also captures ENSO warm-phase events that occur prior to the beginning of the gridded SST product, but that are noted in the historical record (e.g., 1857–59; 1867–69 CE) [*Quinn et al.*, 1987]. Prior to the instrumental
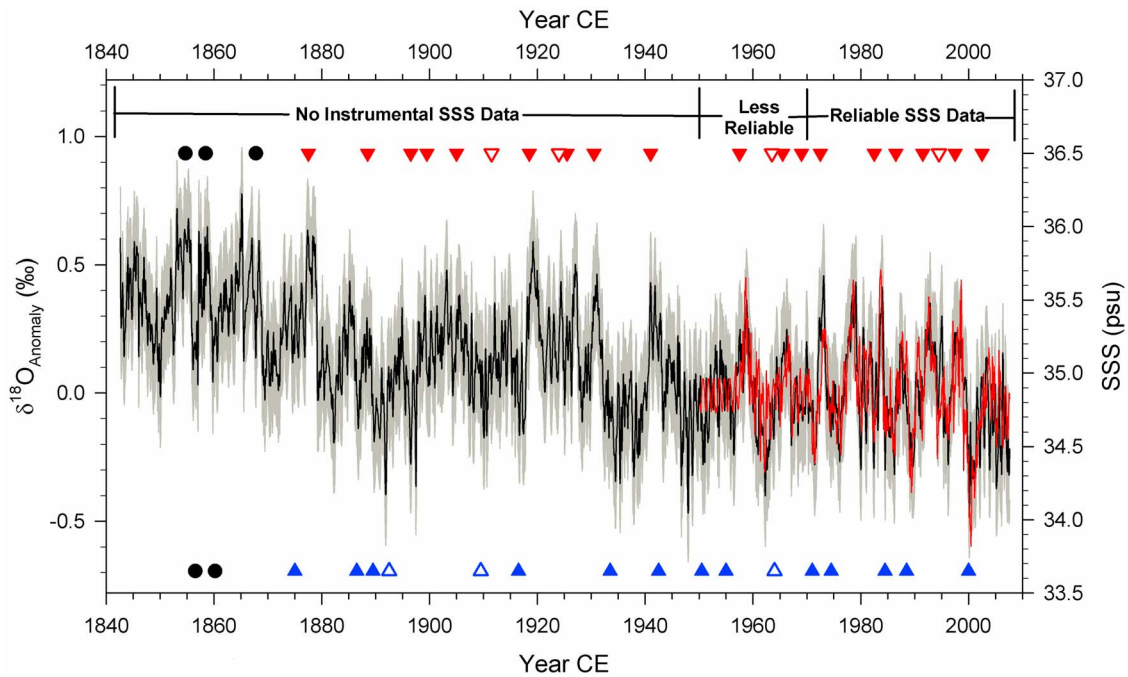
Figure 7. SSS reconstruction from SBV coral δ^{18}O (black) with ± 0.35 psu error cloud (1σ, gray). Our reconstructed salinity record is plotted with instrumental SSS (red), demonstrating the skill of our SSS reconstruction (post-1970), as well as the paucity of instrumental SSS data pre-1970. We mark moderate to strong ENSO warm-phase (solid red triangles) and cool-phase (solid blue triangles) events identified in the instrumental, as well as in our reconstruction. Open triangles indicate ENSO warm-phase (red) and cool-phase (blue) events that occur in the instrumental record, but are not identified in the coral reconstruction. Black circles indicate both ENSO warm and cool-phase events identified by our coral-SSS reconstruction in the pre-instrumental period.

record, accounts of ENSO cool-phase events are much sparser than those of warm-phase events. Our reconstruction identifies two cool-phase events prior to 1870, at 1856 and 1860 CE, which are not widely observed in the historical record [*Ortlieb*, 2000; *Quinn et al.*, 1987].

3.3. Reproducibility of Proxy-Derived SSS Variations

[22] We applied the transfer function (equation (1)) to coral δ^{18}O$_{anomaly}$ variations from Malo Channel, Vanuatu (MCV) to reconstruct salinity at a second location in Vanuatu back to 1939 CE, which we then used as a replication study for the SBV reconstructions (Figure 8a). The δ^{18}O record from MCV was only used back to 1939 because of sampling related issues, recently highlighted by *DeLong et al.* [2007]. The correlation for reconstructed MCV and instrumental SSS is 0.62 (p < 0.01) over their common period 1970–1991 CE. Coral δ^{18}O variability at SBV and MCV, viewed in terms of SSS variability, exhibit a correlation of 0.45 (p > 0.01) over the period covering the entire MCV record, 1939–1991 CE. The mean reconstructed SSS values for SBV and MCV are 34.92 $\pm$ 0.31 and 34.92 $\pm$ 0.29 psu, respectively. These are not significantly different from each other or the instrumental record, which has a mean of 34.87 $\pm$ 0.27 psu. Variations in these coral δ^{18}O records primarily reflect regional salinity variations driven by ENSO-related changes in the SPCZ and its associated salinity front. These correlations in coral skeletal geochemistry across 120 km of ocean provide additional evidence of the robustness of the coral SSS proxy at Vanuatu

as a monitor of the regional response of the surface ocean to ENSO forcing in this region.

3.4. Causes of Interdecadal Scale Variability at SBV

[23] Here we investigate the possible drivers of the interdecadal variability identified by SSA on the δ^{18}O$_{anomaly}$ time series, a proxy for SSS. Changes in SSS can be attributed to a change in the P-E balance of the region or advection of water masses with different SSS signatures. SBV rainfall variability is controlled mainly by the SPCZ, which is influenced by the Interdecadal Pacific Oscillation (IPO) on decadal to interdecadal time scales [*Salinger et al.*, 2001, *Folland et al.*, 2002]. SSA of a rainfall record derived from rain gauge data at Vanuatu over the period 1905–2011 [*Lawrimore et al.*, 2011; P. Masale, personal communication, 2011] resulted in a peak of variability centered at 16.7 years, which accounts for the largest percentage of variability in the record. There is a significant negative correlation of -0.52 (p < 0.05) between the SSA reconstruction of decadal rainfall and decadal δ^{18}O variability (Figure S3). We are unable to use SSA to correlate the interdecadal variability in precipitation to that in SSS due to the short length of the instrumental SSS record, thus we can only speculate that interdecadal variations in rainfall may be driving interdecadal coral δ^{18}O variations at SBV.

[24] An additional possible driver of decadal-scale SSS variability is the advection of water with different SSS signatures into the SBV region. The South Equatorial Current (SEC) flows westward and breaks up into several smaller
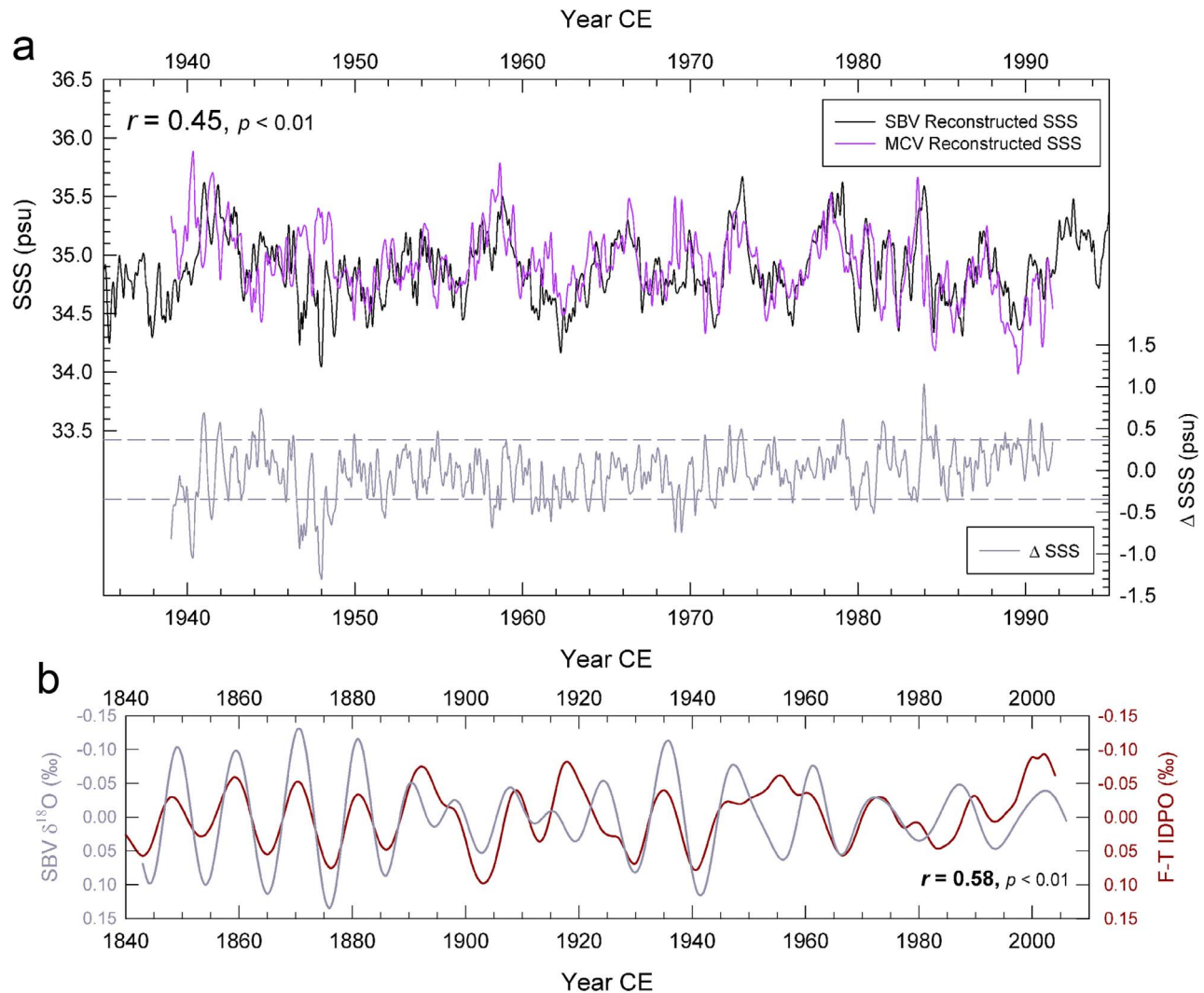
Figure 8. Comparison between SBV coral record and other western Pacific coral records. (a) Our reconstructed SSS time series (black) compared to an SSS reconstruction calculated by applying our $\delta^{18}O$ -SSS transfer function to the $\delta^{18}O$ data from Malo Channel, Vanuatu (purple) [*Kilbourne et al.*, 2004]. The two records agree well, given their separation by 120 km of open-ocean. Dashed horizontal lines indicate the 1σ error associated with the salinity reconstruction (± 0.35psu). (b) SBV $\delta^{18}O$ record (gray) compared to the F-T IDPO (maroon) [*Linsley et al.*, 2008], both records are annually averaged and 8–16 year bandpass filtered. The records have a significant ($p < 0.01$) correlation of $r = 0.58$ over their common period of 1843–2004 CE. While the decadal-scale SSA reconstruction (Figure 5d) varies in amplitude, it is in phase with the decadal-scale filtered record, which gives us confidence in the 8–16 year filtered record and its corresponding correlation with the F-T IDPO.

jets as it encounters the many Pacific islands and reefs [*Webb*, 2000]. Additionally, vertical mixing of the ocean driven by changes in surface winds may draw different water massed up to the surface resulting in SSS variability [*Webb*, 2000]. We speculate that some of the observed interdecadal scale SSS variability at SBV is attributable to the advection of different water masses, possibly as shifts in the surface currents that pass by SBV. Variability in local rainfall at Vanuatu (Figure S3) contributes to the decadal variability in SSS, but changes in ocean currents are likely a main driver. Additional long proxy records of Pacific decadal variability are needed to further understand and distinguish these possibilities.

3.5. Comparison With Other Records and Indices of Pacific Decadal Variability

[25] We investigated the idea that the decadal variability in the SBV coral record reflects decadal-scale movement of the SPCZ by comparing the SBV $\delta^{18}O_{anomaly}$ record to coral records from Fiji and Tonga (F-T), and more specifically, to the reconstructed Fiji-Tonga Interdecadal-Decadal Pacific Oscillation (F-T IDPO) [*Linsley et al.*, 2008], and found that the records have a correlation of 0.58 ($p < 0.01$), and a shared variance of 34% (Figure 8b). We further investigated the correlation between the SBV $\delta^{18}O_{anomaly}$ record and F-T by looking at the correlations between SBV and the five

individual filtered coral records in the F-T composite. Correlations range from a high of 0.62 ($p < 0.01$) between SBV and core TH1 to a low of 0.29 ($p < 0.01$) between SBV and core TNI2. The correlation with the F-T IDPO record(s) and the strength of the decadal variability in our reconstructed SSS time series demonstrates that Vanuatu is a location well suited for examining and understanding Pacific decadal climate variability, and that the decadal variability is regional in extent.

[26] We compared the SSA interdecadal reconstruction of SBV $\delta^{18}O_{anomaly}$ to a commonly used index of Pacific decadal variability, the Pacific Decadal Oscillation (PDO) index [*Mantua et al.*, 1997] over their common period, 1900–2007 CE. We calculated an insignificant correlation ($r = 0.15$, $p > 0.1$), indicating a shared variance of only 2% between the records. We also compared the SBV $\delta^{18}O_{anomaly}$ record with the Interdecadal Pacific Oscillation [*Power et al.*, 1999; *Folland et al.*, 2002], an index of Pacific-wide interdecadal variability, and found an insignificant correlation ($r = 0.13$, $p > 0.1$). This low correlation likely arises because the IPO time series represents the second EOF of global SSTs [*Parker et al.*, 2007, Figure 3], and the SBV $\delta^{18}O_{anomaly}$ record is dominated by SSS variability. In order to make a comparison between SBV and the IPO that is the same as the comparison made between the IPO and the F-T IDPO [*Linsley et al.*, 2008], we compared our data, treated the same as the F-T IDPO data, to the IPO index from *Folland et al.*, [2002], and again found an insignificant correlation ($r = 0.16$, $p > 0.1$). Given the correlation between SBV and the F-T IDPO ($r = 0.58$, $p < 0.01$), it is clear that the locations share some interdecadal variability, but not necessarily variability driven by the IPO. Because the SBV $\delta^{18}O$ record is predominantly driven by SSS at greater than annual timescales, it perhaps should not be surprising that the Vanuatu SSS proxy does not match well with a basin-wide Pacific SST reconstruction that defines the IPO. The fact that coral records from Fiji-Tonga [*Linsley et al.*, 2008] more strongly correlate with the SST-based IPO index than the Vanuatu coral record implies a greater influence of SST and/or a stronger covariation between SST and SSS at Fiji-Tonga than at Vanuatu.

[27] The SBV and F-T IDPO records agree better prior to 1940 than after, suggesting similar surface currents reached all three locations during this earlier period. Changes in the surface water circulation post-1940 likely are responsible for the divergence observed in the coral records at Vanuatu and Fiji-Tonga. Additional data, such as radiocarbon determinations, are needed to further evaluate these proposed changes in surface circulation.

4. Conclusions

[28] ENSO-driven changes in SSTA in the central Pacific region (Niño 3.4) are strongly correlated with observed SSS changes at Vanuatu. Furthermore, the observed changes in SSS are well captured by $\delta^{18}O$ variations recorded in a *Porites lutea* coral head from Sabine Bank, Vanuatu over their period of overlap with the instrumental SSS record (1970–2007 CE). A robust transfer function between coral $\delta^{18}O_{anomaly}$ and SSS, as demonstrated by a successful calibration-verification exercise, was developed at Vanuatu

and used to create a coral-based proxy record of SSS variations extending from 1842 to 2007 CE at SBV and from 1939 to 1991 CE at MCV. The strong reproducibility between the coral $\delta^{18}O$ records from these two localities, which are separated by 120 km of ocean, provides evidence that corals in this region are recording regional changes in salinity. Good agreement of SBV interdecadal variability with the F-T IDPO index pre-1940 further supports the idea of a regional SSS signal, which is likely driven by ENSO-related changes in the SPCZ and the migration of a salinity front. A prominent trend toward freshening of 0.70 ± 0.42 psu is observed and may be attributed to advection of less saline water into the region over time. Additionally, ENSO warm (cool) phase events identified in the instrumental SST record correspond to large positive (negative) salinity excursions, and most importantly, ENSO events prior to the instrumental record are identified in our reconstruction. We observe strong decadal variability in the reconstructed SSS time series (~14 year period), and speculate that local rainfall variability as well as the advection of different water masses near SBV may be influencing SSS on this time scale. Longer proxy records of SSS variations are needed to constrain ENSO and SPCZ changes in the southwest Pacific further and to provide estimates of natural variability in the tropical climate system on decadal to century timescales.

References

Bacastow, R. B., C. D. Keeling, T. J. Lueker, M. Wahlen, and W. G. Mook (1996), The ^{13}C Suess effect in the world surface oceans and its implications for oceanic uptake of CO_2: Analysis of observations at Bermuda, *Global Biogeochem. Cycles*, 10, 335–346, doi:10.1029/96GB00192.

Bjerknes, J. (1969), Atmospheric teleconnections from the equatorial Pacific, *Mon. Weather Rev.*, 97, 163–172, doi:10.1175/1520-0493 (1969)097<0163:ATFTEP>2.3.CO;2.

Brown, J., A. W. Tudhope, M. Collins, and H. V. McGregor (2008), Mid-Holocene ENSO: Issues in quantitative model-proxy data comparisons, *Paleoceanography*, 23, PA3202, doi:10.1029/2007PA001512.

Carton, J. A., and B. S. Giese (2008), A reanalysis of ocean climate using Simple Ocean Data Assimilation (SODA), *Mon. Weather Rev.*, 136, 2999–3017, doi:10.1175/2007MWR1978.1.

Cole, J. E., and R. G. Fairbanks (1990), The Southern Oscillation recorded in the $\delta^{18}O$ of corals from Tarawa Atoll, *Paleoceanography*, 5, 669–683, doi:10.1029/PA005i005p00669.

Cravatte, S., T. Delcroix, D. Zhang, M. J. McPhaden, and J. Leloup (2009), Observed freshening and warming of the western Pacific Warm Pool, *Clim. Dyn.*, 33, 565–589, doi:10.1007/s00382-009-0526-7.

Delcroix, T., S. Cravatte, and M. J. McPhaden (2007), Decadal variations and trends in the tropical Pacific sea surface salinity since 1970, *J. Geophys. Res.*, 112, C03012, doi:10.1029/2006JC003801.

Delcroix, T., G. Alory, S. Cravatte, T. Corrège, and M. J. McPhaden (2011), A gridded sea surface salinity data set for the tropical Pacific with

sample applications (1950–2008), *Deep Sea Res., Part I*, 58, 38–48, doi:10.1016/j.dsr.2010.11.002.

DeLong, K. L., T. M. Quinn, and F. W. Taylor (2007), Reconstructing twentieth-century sea surface temperature variability in the southwest Pacific: A replication study using multiple coral Sr/Ca records from New Caledonia, *Paleoceanography*, 22, PA4212, doi:10.1029/2007PA001444.

DeLong, K. L., T. M. Quinn, C.-C. Shen, and K. Lin (2010), A snapshot of climate variability at Tahit at 9.5 ka using a fossil coral from IODP Expedition 310, *Geochem. Geophys. Geosyst.*, 11, Q06005, doi:10.1029/2009GC002758.

Dunbar, R. B., and G. M. Wellington (1981), Stable isotopes in a branching coral monitor seasonal temperature variation, *Nature*, 293, 453–455, doi:10.1038/293453a0.

Evans, M. N., M. A. Cane, D. P. Schrag, A. Kaplan, B. K. Linsley, R. Villalba, and G. M. Wellington (2001), Support for tropically driven Pacific decadal variability based on paleoproxy evidence, *Geophys. Res. Lett.*, 28(19), 3689–3692, doi:10.1029/2001GL013223.

Fairbanks, R. G., and R. K. Matthews (1978), The marine oxygen isotope record in Pleistocene coral, Barbados, West Indies, *Quat. Res.*, 10, 181–196, doi:10.1016/0033-5894(78)90100-X.

Fairbanks, R. G., M. N. Evans, J. L. Rubenstone, R. A. Mortlock, K. Broad, M. D. Moore, and C. D. Charles (1997), Evaluating climate indices and their geochemical proxies measured in corals, *Coral Reefs*, 16, S93–S100, doi:10.1007/s003380050245.

Folland, C. K., J. A. Renwick, M. J. Salinger, and A. B. Mullan (2002), Relative influences of the Interdecadal Pacific Oscillation and ENSO and the South Pacific Convergence Zone, *Geophys. Res. Lett.*, 29(13), 1643, doi:10.1029/2001GL014201.

Gouriou, Y., and T. Delcroix (2002), Seasonal and ENSO variations of the sea surface salinity and temperature in the South Pacific Convergence Zone during 1976–2000, *J. Geophys. Res.*, 107(C12), 3185, doi:10.1029/2001JC000830.

Gu, D., and S. G. H. Philander (1997), Interdecadal climate fluctuations that depend on exchanges between the tropics and extratropics, *Science*, 275, 805–807, doi:10.1126/science.275.5301.805.

Held, I. M., and B. J. Soden (2006), Robust response of the hydrologic cycle to global warming, *J. Clim.*, 19, 5686–5699, doi:10.1175/JCLI3990.1.

Hereid, K. A., Quinn, T. M., Taylor, F. W., Shen, C., Banner, J. L. (2010), ENSO variability during the Little Ice Age from the perspective of a long coral record from the Western Pacific Warm Pool, Abstract PP43B-1680 presented at 2010 Fall meeting, AGU, San Francisco, Calif., 13–17 Dec.

Juillet-Leclerc, A., S. Thiria, P. Naveau, T. Delcroix, N. Le Bec, D. Blamart, and T. Corrège (2006), SPCZ migration and ENSO events during the 20th century as revealed by climate proxies from a Fiji coral, *Geophys. Res. Lett.*, 33, L17710, doi:10.1029/2006GL025950.

Kiladis, G. N., H. von Storch, and H. van Loon (1989), Origin of the South Pacific Convergence Zone, *J. Clim.*, 2, 1185–1195, doi:10.1175/1520-0442(1989)002<1185:OOTSPC>2.0.CO;2.

Kilbourne, K. H., T. M. Quinn, F. W. Taylor, T. Delcroix, and Y. Gouriou (2004), El Niño–Southern Oscillation–related salinity variations recorded in the skeletal geochemistry of a *Porites* coral from Espiritu Santo, Vanuatu, *Paleoceanography*, 19, PA4002, doi:10.1029/2004PA001033.

Land, L. S., J. C. Lang, and D. J. Barnes (1975), Extension rate: A primary control on the isotopic control of West Indian (Jamaican) scleractinian reef coral skeletons, *Mar. Biol.*, 33, 221–233, doi:10.1007/BF00390926.

Lawrimore, J. H., M. J. Menne, B. E. Gleason, C. N. Williams, D. B. Wuertz, R. S. Vose, and J. Rennie (2011), An overview of the Global Historical Climatology Network monthly mean temperature data set, version 3, *J. Geophys. Res.*, 116, D19121, doi:10.1029/2011JD016187.

Le Bec, N., A. Juillet-Leclerc, T. Corrège, D. Blamart, and T. Delcroix (2000), A coral $\delta^{18}O$ record of ENSO driven sea surface salinity variability in Fiji (south–western tropical Pacific), *Geophys. Res. Lett.*, 27, 3897–3900, doi:10.1029/2000GL011843.

Linsley, B. K., G. M. Wellington, and D. P. Schrag (2000), Decadal sea surface temperature variability in the subtropical south Pacific from 1726–1997 A.D, *Science*, 290, 1145–1148, doi:10.1126/science.290.5494.1145.

Linsley, B. K., A. Kaplan, Y. Gouriou, J. Salinger, P. B. deMenocal, G. M. Wellington, and S. S. Howe (2006), Traching the extent of the South Pacific Convergence Zone since the early 1600 s, *Geochem. Geophys. Geosyst.*, 7, Q05003, doi:10.1029/2005GC001115.

Linsley, B. K., P. Zhang, A. Kaplan, S. S. Howe, and G. M. Wellington (2008), Interdecadal-decadal climate variability from multicoral oxygen isotope records in the South Pacific Convergence Zone region since 1650 A.D, *Paleoceanography*, 23, PA2219, doi:10.1029/2007PA001539.

Mantua, N. J., S. R. Hare, Y. Zhang, J. M. Wallace, and R. C. Francis (1997), A Pacific interdecadal climate oscillation with impacts on salmon production, *Bull. Am. Meteorol. Soc.*, 78, 1069–1079, doi:10.1175/1520-0477(1997)078<1069:APICOW>2.0.CO;2.

McConnaughey, T. (1989), ^{13}C and ^{18}O isotopic disequilibrium in biological carbonates: I. Patterns, *Geochim. Cosmochim. Acta*, 53, 151–162, doi:10.1016/0016-7037(89)90282-2.

McCreary, J., and P. Lu (1994), Interaction between the subtropics and equatorial ocean circulation- the subtropical cell, *J. Phys. Oceanogr.*, 24, 466–497.

McPhaden, M. J., and D. Zhang (2002), Slowdown of the meridional overturning circulation in the upper Pacific Ocean, *Nature*, 415, 603–608, doi:10.1038/415603a.

Morimoto, M., O. Abe, H. Kayanne, N. Kurita, E. Matsumoto, and N. Yoshida (2002), Salinity records for the 1997–98 El Niño from Western Pacific corals, *Geophys. Res. Lett.*, 29(11), 1540, doi:10.1029/2001GL013521.

Newman, M., G. P. Compo, and M. A. Alexander (2003), ENSO-forced variability of the Pacific Decadal Oscillation, *J. Clim.*, 16, 3853–3857, doi:10.1175/1520-0442(2003)016<3853:EVOTPD>2.0.CO;2.

Ortlieb, L. (2000), The documented historical record of El Niño events in Peru: An update of the Quinn record (sixteenth through nineteenth centuries), in *El Niño and the Southern Oscillation: Multiscale Variability and Global and Regional Impacts*, edited by H. F. Diaz and V. Markgraf, pp. 207–250, Cambridge Univ. Press, Cambridge, U. K.

Paillard, D., L. Labeyrie, and P. Yiou (1996), Macintosh program performs time series analysis, *Eos Trans. AGU*, 77, 379, doi:10.1029/96EO00259.

Parker, D., C. Folland, A. Scaife, J. Knight, A. Colman, P. Baines, and B. Dong (2007), Decadal to multidecadal variability and the climate change background, *J. Geophys. Res.*, 112, D18115, doi:10.1029/2007JD008411.

Power, S., T. Casey, C. Folland, A. Colman, and V. Mehta (1999), Interdecadal modulation of the impact of ENSO on Australia, *Clim. Dyn.*, 15, 319–324, doi:10.1007/s003820050284.

Quinn, T. M., and D. E. Sampson (2002), A multiproxy approach to reconstructing sea surface conditions using coral skeleton geochemistry, *Paleoceanography*, 17(4), 1062, doi:10.1029/2000PA000528.

Quinn, W. H., V. T. Neal, and S. E. Antunez de Maylo (1987), El Nino occurences over the past four and a half centuries, *J. Geophys. Res.*, 92, 14,449–14,461, doi:10.1029/JC092iC13p14449.

Quinn, T. M., T. J. Crowley, F. W. Taylor, C. Henin, P. Joannot, and Y. Join (1998), A multi-century stable isotope record from a New Caledonia coral: Interannual and decadal sea surface temperature variability in the southwest Pacific since 1657 A.D, *Paleoceanography*, 13, 412–426, doi:10.1029/98PA00401.

Rasmusson, E. M., and T. H. Carpenter (1982), Variations in tropical sea surface temperature and surface wind fields associated with the Southern Oscillation/El Niño, *Mon. Weather Rev.*, 110, 354–384, doi:10.1175/1520-0493(1982)110<0354:VITSST>2.0.CO;2.

Rayner, N. A., D. E. Parker, E. B. Horton, C. K. Folland, L. V. Alexander, D. P. Rowell, E. C. Kent, and A. Kaplan (2003), Global analyses of sea surface temperature, sea ice, and night marine air temperature since the late nineteenth century, *J. Geophys. Res.*, 108(D14), 4407, doi:10.1029/2002JD002670.

Rayner, N. A., P. Brohan, D. E. Parker, C. K. Folland, J. J. Kennedy, M. Vanicek, T. J. Ansell, and S. F. B. Tett (2006), Improved analysis of changes and uncertainties in sea surafe temperature measures in situ since the mid-nineteenth century: HadSST2 dataset, *J. Clim.*, 19, 446–469, doi:10.1175/JCLI3637.1.

Reverdin, G., S. Morisset, J. Boutin, and N. Martin (2012), Rain-induced variability of near sea-surface T and S from drifter data, *J. Geophys. Res.*, 117, C02032, doi:10.1029/2011JC007549.

Ropelewski, C. F., and M. S. Halpert (1987), Global and regional scale precipitation patterns associated with the El Niño/Southern Oscillation, *Mon. Weather Rev.*, 115, 1606–1626, doi:10.1175/1520-0493(1987)115<1606:GARSPP>2.0.CO;2.

Salinger, M. J., J. A. Renwick, and A. B. Mullan (2001), Interdecdal Pacific Oscillation and South Pacific Climate, *Int. J. Clim.*, 21, 1705–1721, doi:10.1002/joc.691.

Singh, A., and T. Delcroix (2011), Estimating the effects of ENSO upon the observed freshening trends of the western tropical Pacific Ocean, *Geophys. Res. Lett.*, 38, L21607, doi:10.1029/2011GL049636.

Swart, P. K., A. M. Szmant, J. W. Porter, R. E. Dodge, J. I. Tougas, and J. R. Southam (2005), The isotopic composition of respired carbon dioxide in scleractinian corals: Implications for cycling of organic carbon in corals, *Geochim. Cosmochim. Acta*, 69, 1495–1509, doi:10.1016/j.gca.2004.09.004.

Thirumalai, K., A. Singh, and R. Ramesh (2011), A MATLAB^{TM} code to perform weighted linear regression with (correlated or uncorrelated) errors in bivariate data, *J. Geol. Soc. India*, 77, 377–380, doi:10.1007/s12594-011-0044-1.

Thompson, D. M., T. R. Ault, M. N. Evans, J. E. Cole, and J. Emile-Geay (2011), Comparison of observed and simulated tropical climate trends using a forward model of coral δ^{18}O, *Geophys. Res. Lett.*, *38*, L14706, doi:10.1029/2011GL048224.

Vecchi, G. A., B. J. Soden, A. T. Wittenburg, I. M. Held, A. Leetmaa, and M. J. Harrison (2006), Weakening of tropical Pacific atmospheric circulation due to anthropogenic forcing, *Nature*, *441*, 73–76, doi:10.1038/nature04744.

Webb, D. J. (2000), Evidence for shallow zonal jets in the South Equatorial Current region of the southwest Pacific, *J. Phys. Oceanogr.*, *30*, 706–720, doi:10.1175/1520-0485(2000)030<0706:EFSZJI>2.0.CO;2.

Weber, J. N., and P. M. J. Woodhead (1971), Diurnal variations in the isotopic composition of dissolved inorganic carbon in seawater from coral reef environments, *Geochim. Cosmochim. Acta*, *35*, 891–902, doi:10.1016/0016-7037(71)90003-2.

Weber, J. N., and P. M. J. Woodhead (1972), Temperature dependence of oxygen-18 concentrations in reef coral carbonates, *J. Geophys. Res.*, *77*, 463–473, doi:10.1029/JC077i003p00463.

Zhang, D., and M. J. McPhaden (2006), Decadal variability of the shallow Pacific meridional overturning circulation: Relation to tropical sea surface temperatures in observations and climate change models, *Ocean Modell.*, *15*, 250–273, doi:10.1016/j.ocemod.2005.12.005.